Langmuir Article

pubs.acs.org/Langmuir


# Enhanced Tumor Cell Isolation by a Biomimetic Combination of E-selectin and anti-EpCAM: Implications for the Effective Separation of Circulating Tumor Cells (CTCs)

Ja Hye Myung,[†,§] Cari A. Launiere,[‡,§] David T. Eddington,[‡] and Seungpyo Hong*[,†,‡]

[†]*Department of Biopharmaceutical Sciences and* [‡]*Department of Bioengineering, University of Illinois, Chicago, Illinois 60612.* [§]*Both authors contributed equally to this work*

*Received December 11, 2009. Revised Manuscript Received January 28, 2010*

The selective detection of circulating tumor cells (CTCs) is of significant clinical importance for the clinical diagnosis and prognosis of cancer metastasis. However, largely because of the extremely low number of CTCs (as low as 1 in $10^9$ hematologic cells) in the blood of patients, effective detection and separation of the rare cells remain a tremendous challenge. Cell rolling is known to play a key role in physiological processes such as the recruitment of leukocytes to sites of inflammation and selectin-mediated CTC metastasis. Furthermore, because CTCs typically express the epithelial-cell adhesion molecule (EpCAM) on the surface whereas normal hematologic cells do not, substrates with immobilized antibody against EpCAM may specifically interact with CTCs. In this article, we created biomimetic surfaces functionalized with P- and E-selectin and anti-EpCAM that induce different responses in HL-60 (used as a model of leukocytes in this study) and MCF-7 (a model of CTCs) cells. HL-60 and MCF-7 cells showed different degrees of interaction with P-/E-selectin and anti-EpCAM at a shear stress of 0.32 dyn/cm$^2$. HL-60 cells exhibited rolling on P-selectin-immobilized substrates at a velocity of $2.26 \pm 0.28$ $\mu$m/s whereas MCF-7 cells had no interaction with the surface. Both cell lines, however, had interactions with E-selectin, and the rolling velocity of MCF-7 cells ($4.24 \pm 0.31$ $\mu$m/s) was faster than that of HL-60 cells ($2.12 \pm 0.15$ $\mu$m/s). However, only MCF-7 cells interacted with anti-EpCAM-coated surfaces, forming stationary binding under flow. More importantly, the combination of the rolling (E-selectin) and stationary binding (anti-EpCAM) resulted in substantially enhanced separation capacity and capture efficiency (more than 3-fold enhancement), as compared to a surface functionalized solely with anti-EpCAM that has been commonly used for CTC capture. Our results indicate that cell-specific detection and separation may be achieved through mimicking the biological processes of combined dynamic cell rolling and stationary binding, which will likely lead to a CTC detection device with significantly enhanced specificity and sensitivity without a complex fabrication process.

## Introduction

Although recent advances in diagnostic and therapeutic methods to treat primary tumors hold promise to decrease the mortality of cancer, the metastasis of cancer still poses a great challenge because patients often relapse.[1−4] Disseminated and circulating tumor cells (DTCs and CTCs, respectively) are known to induce secondary tumor formation at sites distant from primary tumors, known as metastasis.[5−7] The process of metastasis is not fully understood, but one of the most plausible mechanisms involves a similar process to leukocyte homing (i.e., a naturally occurring cell-rolling process).[8] Rolling cells then firmly attach to the endothelial layers, followed by transmigration through the endothelium (diapedesis) to form secondary tumors.[9] Thus, research efforts on the diagnosis and prognosis of metastatic cancer have been concentrated on the detection of DTCs in bone marrow (BM) and CTCs in blood.[10] The detection of DTCs for prognosis studies along with therapeutic treatments require repeated samplings of BM that are invasive, time-consuming, and often painful for the patient.[11,12] Consequently, the effective detection of CTCs in the peripheral blood of cancer patients holds promise as an alternative because of its minimally invasive and easy sampling procedures (i.e., blood drawing). However the clinical use of CTCs has not yet been implemented in routine clinical practice because CTCs are extremely rare and are estimated to be in the range of 1 tumor cell in the background of $10^6-10^9$ normal blood cells.[13,14]

*All correspondence should be addressed to Prof. Seungpyo Hong, Department of Biopharmaceutical Sciences, College of Pharmacy, The University of Illinois at Chicago, 833 S. Wood Street, Room 335, Chicago, Illinois 60612.

(1) Karnon, J.; Kerr, G. R.; Jack, W.; Papo, N. L.; Cameron, D. A. Health care costs for the treatment of breast cancer recurrent events: estimates from a UK-based patient-level analysis. *Br. J. Cancer* **2007**, *97*, 479−485.

(2) Dong, F.; Budhu, A. S.; Wang, X. W. Translating the metastasis paradigm from scientific theory to clinical oncology. *Clin. Cancer Res.* **2009**, *15*, 2588−2593.

(3) Pepper, M. S. Lymphangiogenesis and tumor metastasis: myth or reality? *Clin. Cancer Res.* **2001**, *7*, 462−468.

(4) Hüsemann, Y.; Geigl, J. B.; Schubert, F.; Musiani, P.; Meyer, M.; Burghart, E.; Forni, G.; Eils, R.; Fehm, T.; Riethmüller, G.; Klein, C. A. Systemic spread is an early step in breast cancer. *Cancer Cell* **2008**, *13*, 58−68.

(5) Chiang, A. C.; Massague, J., Molecular basis of metastasis. *N. Engl. J. Med.* **2008**, *359*, 2814−2823.

(6) Cristofanilli, M.; Budd, G. T.; Ellis, M. J.; Stopeck, A.; Matera, J.; Miller, M. C.; Reuben, J. M.; Doyle, G. V.; Allard, W. J.; Terstappen, L. W. M. M.; Hayes, D. F. Circulating tumor cells, disease progression, and survival in metastatic breast cancer. *N. Engl. J. Med.* **2004**, *351*, 781−791.

(7) Paget, S. The distribution of secondary growths in cancer of the breast. 1889. *Cancer Metastasis Rev.* **1989**, *8*, 98−101.

(8) Mantovani, A.; Allavena, P.; Sica, A.; Balkwill, F. Cancer-related inflammation. *Nature* **2008**, *454*, 436−44.

(9) Mackay, C. R. Moving targets: cell migration inhibitors as new anti-inflammatory therapies. *Nat. Immunol.* **2008**, *9*, 988−998.

(10) Riethdorf, S.; Pantel, K. Disseminated tumor cells in bone marrow and circulating tumor cells in blood of breast cancer patients: current state of detection and characterization. *Pathobiology* **2008**, *75*, 140−148.

(11) Alix-Panabieres, C.; Muller, V.; Pantel, K. Current status in human breast cancer micrometastasis. *Curr. Opin. Oncol.* **2007**, *19*, 558−563.

(12) Lacroix, M. Significance, detection and markers of disseminated breast cancer cells. *Endocr.-Relat. Cancer* **2006**, *13*, 1033−1067.

(13) Pantel, K.; Otte, M. Occult micrometastasis: enrichment, identification and characterization of single disseminated tumour cells. *Semin. Cancer Biol.* **2001**, *11*, 327−337.

(14) Zieglschmid, V.; Hollmann, C.; Bocher, O. Detection of disseminated tumor cells in peripheral blood. *Crit. Rev. Clin. Lab. Sci.* **2005**, *42*, 155−196.

To date, most methods of CTC detection are based on immunofluorescence labeling using CTC markers such as the epithelial cell adhesion molecule (EpCAM).[10,15] Recent progress in this field includes the development of an automated enrichment and immunocytochemical detection system for CTCs (CellSearch, Veridex, LLC) that has been approved by the Food and Drug Administration (FDA) for clinical use in metastatic breast cancer patients.[16,17] Although reliable and stable, the CellSearch system has limitations such as complicated sample processing with additional steps needed for plasma removal and magnetic antibody labeling and limited sensitivity with a median 1.2 cells/mL detected from patients with metastatic cancer. Other promising technology for CTC detection and isolation has recently been published by Nagrath et al. using a microfluidic device containing 78 000 anti-EpCAM-coated microposts, which increases its sensitivity and specificity for CTC capture.[18] The CTC chip does not require multiple processing steps in sample preparation and has shown enhanced sensitivity as compared to CellSearch with a median of 67 cells/mL detected from whole blood samples of patients under comparable conditions.[19] The combined effect of anti-EpCAM-based specificity and the micropost-enhanced hydrodynamic efficiency enabled a capture of over 60%. However, the enhanced hydrodynamic efficiency relying on the microposts limits the utility of the device at higher flow rates, where a significant decrease in the capture efficiency has been observed.

The formation of transient ligand−receptor interactions commonly occurs between cells flowing in the blood and the vascular endothelium; this physiological process is known as cell rolling.[20] Cell rolling plays a key role in biologically important processes such as the recruitment of leukocytes to sites of inflammation, the homing of hematopoietic progenitor cells, and CTC-induced metastasis. This behavior is typically mediated by dynamic interactions between selectins (E- and P-selectins) on the vascular endothelial cell surface and membrane ligands on the carcinoma cell surface. Endothelial (E)-selectin (CD62E) is particularly noteworthy in disease by virtue of its expression on activated endothelium and on bone−skin microvascular linings, and many studies point to the key role played by E-selectin in being involved in the adhesion and homing of various types of cancer cells such as prostate,[21] breast,[22,23] and colon[24] carcinoma cells. Thus, tumor-cell separation based on the selectin-mediated cell rolling behavior is being pursued because it mimics a physiological process and eliminates labeling and label removal steps that are necessary for other immune-labeling detection methods.[25] Recently, a tube-type flow chamber that is co-immobilized with E-selectin and tumor necrosis factor-related apoptosis-inducing ligand (TRAIL) achieved concurrent dual functions of inducing rolling and apoptosis of various cell lines.[26] However, given that a large class of cells, including leukocytes, platelets, neutrophils, mesenchymal and hematopoietic stem cells, and metastatic cancer cells, all exhibit rolling on selectins, detection that is solely based on cell rolling has limitations for achieving sufficient specificity, which has hindered the translation of the technology to a clinically significant device.

The specific capturing and potential enrichment of CTCs using anti-EpCAM and selectin, respectively, inspired a biofunctionalized surface that mimics biological complexity and may detect and isolate target cells at a greater sensitivity and specificity. This concept is supported by the initial physiological interactions between CTCs and endothelium in the bloodstream, which include concurrent rolling and stationary binding steps. Toward this aim, we investigated the following: (i) two proteins with distinct biofunctions (selectin to induce rolling and anti-EpCAM to capture target cells statically) can be co-immobilized; (ii) a combined rolling and stationary binding can be induced by the mixture of the proteins; and (iii) the biomimetic combination enhances the overall capture efficiency of the surface. In this article, these are tested using biofunctional surfaces with immobilized selectins and anti-EpCAM. The surfaces are characterized by X-ray photoelectron scattering (XPS) and fluorescence microscopy using fluorophore-conjugated antibodies. As a proof-of-concept study for the hypothesis of enhanced separation capacity and capture efficiency using protein mixtures, the surfaces are tested using in vitro cell lines (MCF-7 cells as a CTC model and HL-60 cells as a leukocyte model) under flow conditions. The effects of the combination of rolling (E-selectin) and stationary binding (anti-EpCAM) on capture efficiency are compared to a surface functionalized solely with anti-EpCAM or selectins. Here we report, for the first time to our knowledge, that a combination of dynamic rolling and stationary binding significantly enhances the capture efficiency of target cells, which holds great promise for developing a simple, effective device for CTC detection.

## Experimental Section

**Materials.** Recombinant human P-selectin/Fc chimera (P-selectin), E-selectin/Fc chimera (E-selectin), antihuman EpCAM/TROP1 polyclonal antibody (anti-EpCAM), fluorescein-conjugated mouse monoclonal antihuman E-selectin (fluorescein-anti-E-selectin), and allophycocyanin (APC)-conjugated mouse monoclonal antihuman EpCAM/TROP1 (APC-anti-EpCAM) were all purchased from R&D systems (Minneapolis, MN). Unconjugated goat anti-human IgG (H + L) was acquired from Pierce Biotechnology, Inc. (Rockford, IL). Epoxy-functionalized

(15) Krivacic, R. T.; Ladanyi, A.; Curry, D. N.; Hsieh, H. B.; Kuhn, P.; Bergsrud, D. E.; Kepros, J. F.; Barbera, T.; Ho, M. Y.; Chen, L. B.; Lerner, R. A.; Bruce, R. H. A rare-cell detector for cancer. *Proc. Natl. Acad. Sci. U.S.A.* **2004**, *101*, 10501−10504.

(16) Danila, D. C.; Heller, G.; Gignac, G. A.; Gonzalez-Espinoza, R.; Anand, A.; Tanaka, E.; Lilja, H.; Schwartz, L.; Larson, S.; Fleisher, M.; Scher, H. I. Circulating tumor cell number and prognosis in progressive castration-resistant prostate cancer. *Clin. Cancer Res.* **2007**, *13*, 7053−7058.

(17) Riethdorf, S.; Fritsche, H.; Muller, V.; Rau, T.; Schindlbeck, C.; Rack, B.; Janni, W.; Coith, C.; Beck, K.; Janicke, F.; Jackson, S.; Gornet, T.; Cristofanilli, M.; Pantel, K. Detection of circulating tumor cells in peripheral blood of patients with metastatic breast cancer: a validation study of the CellSearch system. *Clin. Cancer Res.* **2007**, *13*, 920−928.

(18) Nagrath, S.; Sequist, L. V.; Maheswaran, S.; Bell, D. W.; Irimia, D.; Ulkus, L.; Smith, M. R.; Kwak, E. L.; Digumarthy, S.; Muzikansky, A.; Ryan, P.; Balis, U. J.; Tompkins, R. G.; Haber, D. A.; Toner, M. Isolation of rare circulating tumour cells in cancer patients by microchip technology. *Nature* **2007**, *450*, 1235−1239.

(19) Maheswaran, S.; Sequist, L. V.; Nagrath, S.; Ulkus, L.; Brannigan, B.; Collura, C. V.; Inserra, E.; Diederichs, S.; Iafrate, A. J.; Bell, D. W.; Digumarthy, S.; Muzikansky, A.; Irimia, D.; Settleman, J.; Tompkins, R. G.; Lynch, T. J.; Toner, M.; Haber, D. A. Detection of mutations in EGFR in circulating lung-cancer cells. *N. Engl. J. Med.* **2008**, *359*, 366−377.

(20) Tedder, T. F.; Steeber, D. A.; Chen, A.; Engel, P. The selectins: vascular adhesion molecules. *FASEB J.* **1995**, *9*, 866−873.

(21) Dimitroff, C. J.; Lechpammer, M.; Long-Woodward, D.; Kutok, J. L. Rolling of human bone-metastatic prostate tumor cells on human bone marrow endothelium under shear flow is mediated by E-selectin. *Cancer Res.* **2004**, *64*, 5261−5269.

(22) Giavazzi, R.; Foppolo, M.; Dossi, R.; Remuzzi, A. Rolling and adhesion of human tumor cells on vascular endothelium under physiological flow conditions. *J. Clin. Invest* **1993**, *92*, 3038−3044.

(23) Yuan, K.; Kucik, D.; Singh, R. K.; Listinsky, C. M.; Listinsky, J. J.; Siegal, G. P. Alterations in human breast cancer adhesion-motility in response to changes in cell surface glycoproteins displaying alpha-L-fucose moieties. *Int. J. Oncol.* **2008**, *32*, 797−807.

(24) Tremblay, P. L.; Huot, J.; Auger, F. A. Mechanisms by which E-selectin regulates diapedesis of colon cancer cells under flow conditions. *Cancer Res.* **2008**, *68*, 5167−5176.

(25) Greenberg, A. W.; Hammer, D. A. Cell separation mediated by differential rolling adhesion. *Biotechnol. Bioeng.* **2001**, *73*, 111−124.

(26) Rana, K.; Liesveld, J. L.; King, M. R. Delivery of apoptotic signal to rolling cancer cells: a novel biomimetic technique using immobilized TRAIL and E-selectin. *Biotechnol. Bioeng.* **2009**, *102*, 1692−1702.

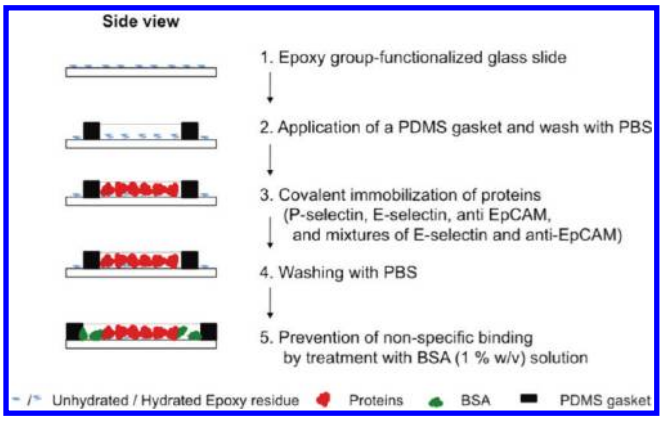


**Figure 1.** Surface functionalization by the immobilization of proteins.

glass surfaces (SuperEpoxy2) were purchased from TeleChem International, Inc. (Sunnyvale, CA). All other chemicals were obtained from Sigma-Aldrich (St. Louis, MO) and used without further purification.

**Surface Functionalization by the Immobilization of Adhesive Proteins.** All individual proteins and/or mixture of P-selectin, E-selectin, and anti-EpCAM were immobilized on epoxy-functionalized glass surfaces. A general scheme of the surface functionalization via protein immobilization is outlined in Figure 1. The coating areas were defined by a polydimethylsiloxane (PDMS) gasket to confine protein solutions in a desired area, resulting in a clear interface between protein-coated and uncoated regions. For the surfaces functionalized with a single protein, 300 $\mu$L of each protein (P-selectin, E-selectin, or anti-EpCAM) at a concentration of 5 $\mu$g/mL in PBS buffer (Cellgro, without $Ca^{2+}$ and $Mg^{2+}$) was added to an approximately 2 $cm^2$ area of a slide defined by a PDMS gasket, followed by incubation at RT for 4 h with constant, gentle shaking on a plate shaker. The PDMS gasket was then removed, and the whole slide surface was washed with PBS three times. Potential nonspecific binding of both protein-coated and uncoated regions was blocked by the final incubation with 1% (w/v) bovine serum albumin (BSA) in PBS buffer (BSA solution). The subsequent experiments using the surfaces were immediately performed or stored in PBS buffer at 4 °C. Additionally, mixtures of E-selectin and anti-EpCAM were immobilized at various ratios under the same condition described above. A fixed concentration of anti-EpCAM at 10 $\mu$g/mL was used with various amounts of E-selectin. The final total weights (in $\mu$g) of anti-EpCAM and E-selectin were 1.5:0, 1.5:0.3, 1.5:1.5, and 1.5:7.5.

**Characterization of Functionalized Surfaces by Fluorescence Microscopy.** The co-immobilization process of anti-EpCAM and E-selectin was characterized using APC-anti-EpCAM and fluorescein-anti-E-selectin, respectively. The surfaces functionalized with P-selectin were explicitly characterized previously.[27] Because neither fluorophore-tagged EpCAM nor fluorescent secondary antibody specific to anti-EpCAM is commercially available, APC-anti-EpCAM was co-immobilized with E-selectin and red fluorescence was observed from the surface. For the detection of E-selectin, anti-EpCAM/E-selectin-immobilized slides were incubated with fluorescein-conjugated anti-E-selectin (25 $\mu$g/mL) at 4 °C for 1 h, followed by a washing step (three times using PBS buffer). All slides were then mounted using Vectashield mounting medium (Vector Laboratories, Inc., Burlingame, CA), and air bubbles in the mounting medium were gently removed by applying pressure to the cover slides. The fluorescence images were taken using an Olympus IX70 inverted microscope equipped with a fluorescence illuminator (IX 70-S1F2, Olympus America, Inc., Center Valley, PA) using a 10× objective, a CCD camera (QImaging Retiga 1300B, Olympus America, Inc.), and filters for FITC (450 nm excitation and 535 nm emission) and APC (560 nm excitation and 645 nm emission). For each image (triplicate for each sample), five regions of equal size were randomly selected, and the total pixel intensity values within these regions were acquired using ImageJ (NIH). The slide treated with the BSA solution was used as the background, and its intensity value was subtracted from all sample slides. The intensities obtained from the protein-mixture-immobilized slides were normalized on the basis of those functionalized with a single protein (anti-EpCAM or E-selectin) to compare the relative amounts.

**Characterization of the Surfaces by X-ray Photoelectron Spectroscopy (XPS).** Protein-immobilized surfaces were characterized by XPS.[27] XPS measurements were performed using an Axis 165 X-ray photoelectron spectrometer (Kratos Analytical, Manchester, U.K.) equipped with a monochromatic Al K$\alpha$ source ($h\nu$ = 1486.6 eV, 150 W) and a hemispherical analyzer. The % mass concentrations were obtained from high-resolution spectra of the C 1s, O 1s, N 1s, and S 2p regions at an X-ray irradiating angle of 30° with a pass energy of 80 eV and a step size of 0.5 eV, carried out on five scans per spectrum.

**Cell Lines.** HL-60 and MCF-7 cells were purchased from ATCC (Manassas, VA). *Discosoma* sp. red fluorescent protein (DsRED)-transfected MCF-7 (DsRED-MCF-7) cells that were transfected using an HIV-1-based lentiviral vector[28] were a generous gift from Prof. William Beck at UIC.

HL-60 cells were cultured in IMDM media supplemented with 20% (v/v) fetal bovine serum (FBS) and 1% (v/v) penicillin/streptomycin in a humidified incubator at 37 °C and 5% $CO_2$. MCF-7 cells and DsRED-MCF-7 cells were cultured in DMEM media that were supplemented with 10% (v/v) FBS and 1% (v/v) penicillin/streptomycin under the same conditions of incubation for HL-60 cells. Prior to cell culturing, to enrich the transfected (fluorescent) cell population, DsRED-MCF-7 cells were isolated from nontransfected MCF-7 cells via the dilution of the cell suspension ($10^3$ cells in 10 mL of medium in a Petri dish) and the selection of the transfected MCF-7 cells using a fluorescence microscope (Olympus IX70). HL-60, MCF-7, and DsRED-MCF-7 cells were prepared by resuspension in their own supplemented media with anti-IgG and were kept on ice during the subsequent cell rolling experiments.[29]

**Flow Chamber Experiments.** A typical flow chamber experiment was performed as follows. A glass slide functionalized by protein immobilization, a gasket (30 mm (L) × 10 mm (W) × 0.25 mm (D), Glycotech, Gaithersburg, MD), and a rectangular parallel plate flow chamber (Glycotech) were assembled in line under vacuum. To observe cellular interactions with the biofunctionalized surfaces, individual cell lines (HL-60 or MCF-7) as well as mixtures of the two cell lines (HL-60 and DsRED-MCF-7) at a concentration between $10^5$ and $10^7$ cells/mL were injected into the flow chamber at various shear stresses (0.08−1.28 dyn/$cm^2$) using a syringe pump (New Era Pump Systems Inc., Farmingdale, NY). Note that, in this flow chamber, a 200 $\mu$L/min flow rate corresponds to 0.32 dyn/$cm^2$ wall shear stress, a 32 $s^{-1}$ wall shear rate, and 80 $\mu$m/s near-wall nonadherent cell velocity according to the Goldman equation.[30]

**Observation of Cellular Responses on Various Functional Surfaces.** Throughout this study, the cellular behaviors on the

(27) Hong, S.; Lee, D.; Zhang, H.; Zhang, J. Q.; Resvick, J. N.; Khademhosseini, A.; King, M. R.; Langer, R.; Karp, J. M. Covalent immobilization of p-selectin enhances cell rolling. *Langmuir* **2007**, *23*, 12261−12268.

(28) Ramezani, A.; Hawley, R. G. Generation of HIV-1-based lentiviral vector particles. *Curr. Protoc. Mol. Biol.* **2002**, Chapter 16, Unit 16 22.

(29) Nilsson, R.; Sjogren, H. O. Antigen-independent binding of rat immunoglobulins in a radioimmunoassay. Solutions to an unusual background problem. *J. Immunol. Methods* **1984**, *66*, 17−25.

(30) Goldman, A. J.; Cox, R. G.; Brenner, H. Slow viscous motion of a sphere parallel to a plane wall--II Couette flow. *Chem. Eng. Sci.* **1967**, *22*, 653−660.

**Table 1. Immunostaining Results of Surfaces Immobilized with E-selectin, anti-EpCAM, and Mixtures of the Two Proteins[a]**

| | anti-EpCAM (1.5 $\mu$g) | E-selectin (1.5 $\mu$g) | anti-EpCAM (1.5 $\mu$g)/ E-selectin (0.3 $\mu$g) | anti-EpCAM (1.5 $\mu$g)/ E-selectin (1.5 $\mu$g) | anti-EpCAM (1.5 $\mu$g)/ E-selectin (7.5 $\mu$g) |
|---|---|---|---|---|---|
| FITC-anti-E-selectin (for E-selectin detection) | | 1 | $0.04 \pm 0.01$ | $0.66 \pm 0.06$ | $1.31 \pm 0.02$ |
| APC-anti-EpCAM (for anti-EpCAM detection) | 1 | | $0.88 \pm 0.31$ | $0.96 \pm 0.70$ | $0.61 \pm 0.31$ |

[a] Note that all the fluorescence intensities were normalized on the basis of the intensities measured on the surfaces with individual proteins.

**Table 2. Atomic Compositions of Functionalized Slides with Various Proteins, as Measured by XPS**

| | control (mass conc %) | E-selectin (mass conc %) | anti-EpCAM (mass conc %) | anti-EpCAM 1.5 $\mu$g/E-selectin 0.3 $\mu$g (mass conc %) | anti-EpCAM 1.5 $\mu$g/E-selectin 1.5 $\mu$g (mass conc %) | anti-EpCAM 1.5 $\mu$g/E-selectin 7.5 $\mu$g (mass conc %) |
|---|---|---|---|---|---|---|
| C 1s | 11.3 | 21.6 | 26.2 | 32.5 | 40.2 | 36.9 |
| N 1s | 0.0 | 5.4 | 2.6 | 3.5 | 4.6 | 6.5 |
| O 1s | 59.7 | 51.9 | 39.2 | 43.3 | 35.5 | 40.7 |
| Si 2p | 29.0 | 21.1 | 32.0 | 20.7 | 19.7 | 15.9 |
| N/C ratio | 0.0 | 0.3 | 0.1 | 0.1 | 0.1 | 0.2 |
| C/O ratio | 0.2 | 0.4 | 0.7 | 0.8 | 1.1 | 0.9 |

various surfaces in the flow chamber were all monitored using the Olympus IX70 microscope, and images were recorded using a CCD camera. Rolling velocities of cells on the immobilized proteins were calculated on the basis of images taken every second for 1 min using ImageJ. Cell rolling was defined when the rolling velocities were less than 50% of the free stream velocity (e.g., slower than 40 $\mu$m/s at a flow rate of 200 $\mu$L/min). Rolling dynamic data was presented as mean ± standard error of the mean (SEM) values of repetitive observations. To confirm the statistical significance between data points, rolling velocities of more than 40 cells per image were tracked independently for at least 5 replicates.

To evaluate the separation of the two cell populations in the mixtures, fluorescent DsRED-MCF-7 cells were used as a CTC model so that they could be easily distinguished from the nonfluorescent leukocyte model (HL-60 cells) in a 50:50 mixture. The surface interactions of the cell mixture on each type of protein and the cell separation at the interface between E-selectin (left) and anti-EpCAM (right)-coated regions were visualized using the fluorescent and bright fields for 1 min. The merged images of the fluorescent and bright fields were taken in the absence of flow.

The DsRED-MCF-7 capture efficiency of the surfaces functionalized with E-selectin/anti-EpCAM combinations was measured as follows. The slides functionalized with different ratios of E-selectin/anti-EpCAM combinations were prepared, and DsRED-MCF-7 cells (suspended in PBS at 2500 cells/mL with anti-IgG) were injected into a flow chamber, followed by repetitive syringe pushing in and withdrawing at 100 $\mu$L/min (0.16 dyn/cm$^2$). The number of captured cells on a predefined area of a protein-immobilized surface was counted using a microscope in each cycle. A cycle consists of forward flow (pushing) for 2.5 min, backward flow (withdrawing) for 2.5 min, and PBS washing for 1 min. As the known number of DsRED-MCF-7 cells perfused into the flow chamber, the number of captured cells could be translated into the capture efficiency (%). The measured capture efficiencies of the protein-mixture-immobilized slides were statistically analyzed by comparing to those of the anti-EpCAM-immobilized slides using one-factor ANOVA, followed by pairwise comparisons among levels of weight for posthoc analyses by Fisher's least significant difference (LSD) tests with 95% simultaneous confidence intervals (SPSS software, Chicago, IL). Prior to the ANOVA test, we also confirmed that all of the capture efficiency data are normally distributed on the basis of both Kolmogorov−Smirnov and Shapiro−Wilk tests using SPSS software. The overall error rate of $p < 0.05$ was considered to be statistically significant and was marked with an asterisk (*) as shown in Figure 6.

## Results

**Confirmation of the Immobilization of E-Selectin, anti-EpCAM, and Combinations of Proteins on Glass Substrates.** Surface functionalization by protein immobilization was confirmed by fluorescence microscopy and XPS, as summarized in Tables 1 and 2, respectively. The commercially available epoxy-terminated slides with a highly reactive coupling efficiency (via amine/hydroxyl/thiol-based chemistries) and low fluorescence background allowed quantitative, reliable surface analyses using the two techniques. The presence of E-selectin on the surface was observed by immunostaining using fluorescein-anti-E-selectin (green fluorescence). APC-anti-EpCAM (red fluorescence) was used instead of nonfluorescent anti-EpCAM to image surface-immobilized anti-EpCAM by fluorescence microscopy. Table 1 summarizes the measured fluorescence intensities of the various bioadhesive surfaces. For the surfaces functionalized with E-selectin/anti-EpCAM mixtures, the measured fluorescence intensities of each fluorophore dictate the compositions of each protein. With an increase in the amount of E-selectin immobilized, the green fluorescence intensity was obviously increased but minimal changes in the red fluorescence intensity were also observed.

The immobilization of anti-EpCAM and/or E-selectin was quantitatively confirmed by an increase in carbon and nitrogen compositions and decreased silicon detection in the underlying glass substrate, as measured by XPS analysis (Table 2). Furthermore, as the amount of immobilized E-selectin in the mixture of anti-EpCAM and E-selectin was increased, the amounts of carbon and nitrogen on the surface were increased with decreased silicon composition. All surfaces immobilized with proteins had a high degree of coverage, as evidenced by the decreased mass composition of silicon. The measured nitrogen content likely corresponds to the degree of protein coverage on the glass surface, which is supported by the increased nitrogen composition when the total number of proteins immobilized was increased.

**Interactions of Cells on Protein-Immobilized Surfaces.** Cell interactions with protein-immobilized surfaces under flow were assessed using a commercially available rectangular parallel-plate flow chamber. A breast cancer cell line, MCF-7, was employed as a CTC model. The rolling behavior of the MCF-7 cells was compared with that of HL-60 cells, a human myeloid leukocytic cell line that expresses a high level of sialyl Lewis X and

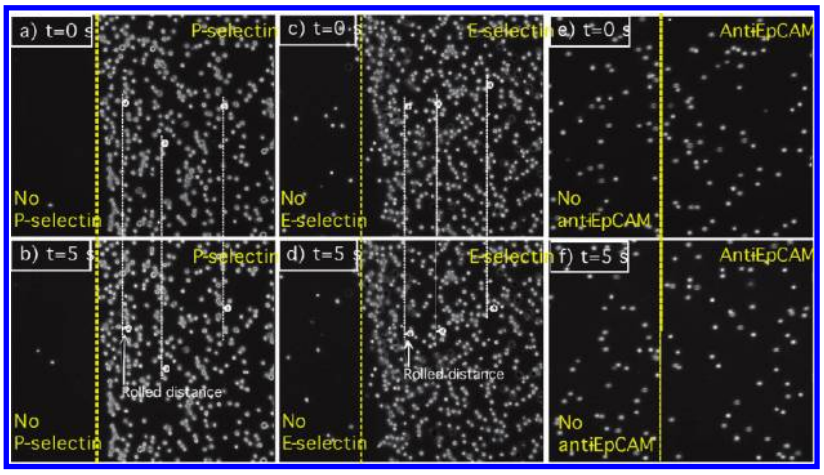


**Figure 2.** Time-course images of HL-60 cells under a shear stress of 0.32 dyn/cm$^2$ on (a, b) P-selectin-, (c, d) E-selectin-, and (e, f) anti-EpCAM-immobilized surfaces. The rolling velocities (mean ± standard error, $n = 200$) of the cells on P-selectin and E-selectin were 2.26 ± 0.28 and 2.12 ± 0.15 $\mu$m/s, respectively, whereas there was no interaction observed between the cells and the anti-EpCAM-coated surface. The cells in images e and f are noninteracting flowing cells. The flow direction of the three sets is from left to right.

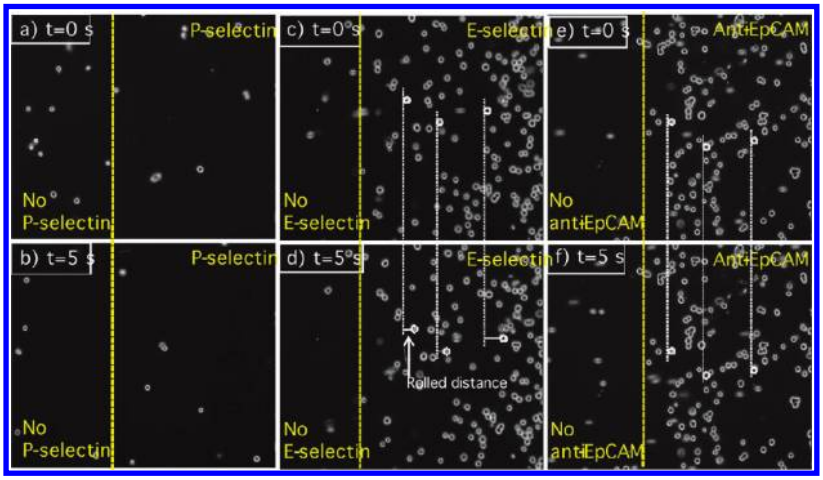


**Figure 3.** Time-course images of MCF-7 cells under shear stress of 0.32 dyn/cm$^2$ on (a, b) P-selectin, (c, d) E-selectin, and (e, f) anti-EpCAM-immobilized surfaces. MCF-7 cells exhibited rolling behavior on the E-selectin-coated surface (4.24 ± 0.31 $\mu$m/s) or were captured on the anti-EpCAM-coated surface. However, there was no interaction observed between cells and the P-selectin-coated surface. The flow direction of the three sets is from left to right. All of the rolling dynamic data is represented as the mean ± standard error ($n = 200$).

exhibits rolling on selectins mediated primarily by P-selectin glycoprotein-1 (PSGL-1).[31,32]

Each set (a and b, c and d, and e and f) in Figure 2 shows HL-60 cells on P-selectin-, E-selectin-, and anti-EpCAM-coated surfaces at $t = 0$ s (a randomly chosen initial recording time during the flow experiment) and 5 s (5 s after the starting time), respectively. Note that the HL-60 cells on the anti-EpCAM-coated slide observed in the images at 0 s were nonadherent cells that were in the main flow but vertically close to the surface. As previously reported, HL-60 cells exhibited stable rolling on both P- and E-selectin-immobilized slides at velocities of 2.26 ± 0.28 and 2.12 ± 0.15 $\mu$m/s, respectively, under 0.32 dyn/cm$^2$ of shear stress. HL-60 cells showed no interactions with immobilized anti-EpCAM, traveling the flow path in the chamber at the speed of the free stream velocity (Figure 2e,f). In contrast, as shown in Figure 3, MCF-7 cells did not interact with immobilized P-selectin but exhibited the rolling response on the E-selectin-coated surfaces. The rolling velocities of MCF-7 on E-selectin-immobilized slides (4.24 ± 0.31 $\mu$m/s) were faster than those of HL-60 (2.12 ± 0.15 $\mu$m/s). It should be noted that the rolling velocities of MCF-7 cells varied between experiments with relatively high standard errors, whereas the velocities of HL-60 cells on E-selectin-immobilized slides were relatively consistent between experiments. Unlike HL-60 cells, however, MCF-7 cells exhibited a strong interaction with immobilized anti-EpCAM slides, rolling very slowly (0.09 ± 0.03 $\mu$m/s) so that they appeared to be stationary on the surface. Additionally, the rolling velocities of HL-60 and MCF-7 cells on E-selectin were measured at four different shear stresses (0.08−1.28 dyn/cm$^2$) as shown in Figure 4. The rolling velocity of MCF-7 cells was significantly increased with an increase in the shear stress (~3.2−8.0 $\mu$m/s) whereas the rolling response of HL-60 cells was less dependent upon the flow-rate change (~1.5−2.3 $\mu$m/s).

**Enhanced Separation of Tumor Cells from Two Cell Populations Using Combinations of anti-EpCAM and E-selectin.** Interactions of mixtures of the two cell lines with various surfaces functionalized with P-selectin, E-selectin, anti-EpCAM,

(31) Kobzdej, M. M.; Leppanen, A.; Ramachandran, V.; Cummings, R. D.; McEver, R. P. Discordant expression of selectin ligands and sialyl Lewis x-related epitopes on murine myeloid cells. *Blood* **2002**, *100*, 4485−4494.

(32) Zou, X.; Shinde Patil, V. R.; Dagia, N. M.; Smith, L. A.; Wargo, M. J.; Interliggi, K. A.; Lloyd, C. M.; Tees, D. F.; Walcheck, B.; Lawrence, M. B.; Goetz, D. J. PSGL-1 derived from human neutrophils is a high-efficiency ligand for endothelium-expressed E-selectin under flow. *Am. J. Physiol. Cell Physiol.* **2005**, *289*, C415−C424.

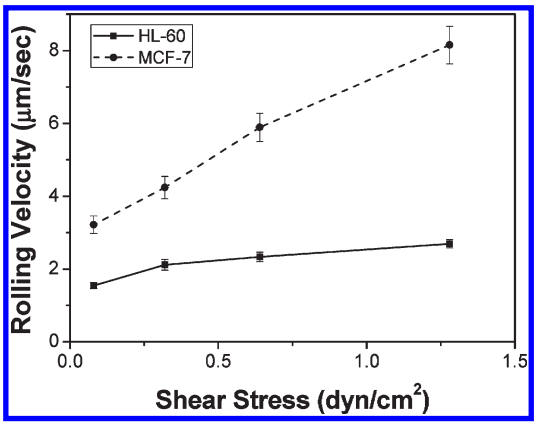


**Figure 4.** Cell rolling velocities of HL-60 and MCF-7 cells on E-selectin-immobilized slides under various shear stresses (0.08, 0.32, 0.64, and 1.28 dyn/cm$^2$). Note that the rolling response of HL-60 cells is minimally affected by an increase in shear stress, whereas MCF-7 cells show rolling that is very dependent upon shear stress. Error bars denote the standard error.

and combinations of E-selectin/anti-EpCAM were observed under flow conditions, as shown in Figure 5. Note that DsRED-MCF-7 cells were used for easy recognition and appeared to be red in all of the images taken on a fluorescence microscope. As shown in Figure 5a, P-selectin induced the rolling of HL-60 but did not interact with DsRED-MCF-7 cells, which is consistent with the results using nontransfected MCF-7 cells as shown in Figure 3. E-selectin, however, caused both cells to roll as presented in Figure 5b. The surface with anti-EpCAM alone induced the stationary adhesion of DsRED-MCF-7 cells exclusively. Although HL-60 cells had no interaction with anti-EpCAM, some of them were still located on the images of the anti-EpCAM-immobilized surface (Figure 5c) but these cells were in the bulk flow and were not captured on the slide. As shown in Figure 5d, the combined but spatially separated E-selectin and anti-EpCAM indeed provided enhanced separation of MCF-7 cells from the cell mixture, compared to the surface functionalized with E-selectin. Both cell types rolled on the E-selectin-coated region (the left-hand side of the image), followed by clear separation of the pure MCF-7 cells in the adjacent anti-EpCAM-coated region (the right-hand side).

**Enhanced Capture of Tumor Cells Using Combinations of anti-EpCAM and E-selectin.** The effect of E-selectin addition to the anti-EpCAM-coated surface was further examined by the quantitative analysis of the capture efficiency of DsRED-MCF-7 cells. Figure 6a,b demonstrates a statistically significant enhancement in capture efficiency with the surface immobilized with the mixtures (anti-EpCAM and E-selectin), as compared to the surface with anti-EpCAM only. As shown in Figure 6a,b, the average number of captured cells by the surfaces with the two proteins was enhanced in an E-selectin concentration-dependent manner. The enhancement of capture efficiency of the surface with E-selectin/anti-EpCAM compared to that with anti-EpCAM alone was observed to be as high as 3-fold.

To evaluate cell capture under various conditions further, a series of experiments in which DsRED-MCF-7 cells (2500 cells/mL of PBS buffer) were spiked with HL-60 (2500 cells/mL of PBS buffer) in the presence of anti-IgG were conducted. The rolling velocity of HL-60 cells was measured at a flow rate of 200 $\mu$L/min (0.32 dyn/cm$^2$). Figure 7 quantitatively presents the capture efficiency of DsRED-MCF-7 cells and rolling velocities of HL-60 on surfaces with co-immobilized E-selectin and anti-EpCAM at various ratios. As the amount of E-selectin in the total

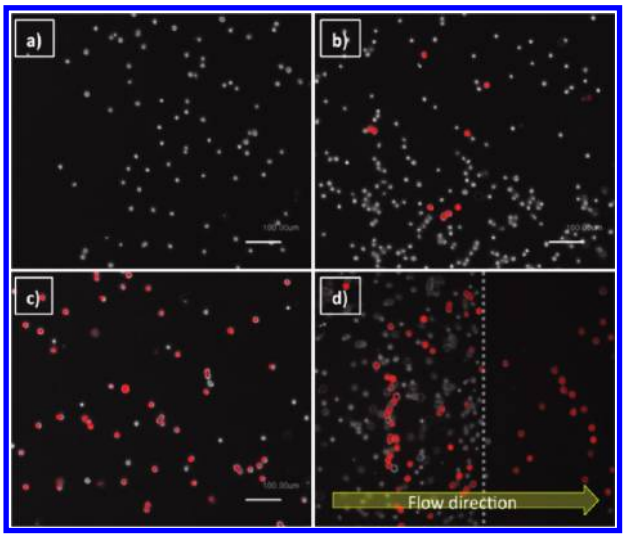


**Figure 5.** Images of HL-60 and DsRED-transfected MCF-7 cells (red cells) on (a) P-selectin-, (b) E-selectin-, (c) anti-EpCAM-, and (d) patterned E-selectin/anti-EpCAM-coated surfaces under a shear stress of 0.32 dyn/cm$^2$. The patterned surface with E-selectin and anti-EpCAM shown in image d achieved an efficient isolation of DsRED-transfected MCF-7 (a CTC model: red cells) cells from the mixture with HL-60 (a leukocyte model: white cells) on the anti-EpCAM-coated region.

immobilized proteins was increased, the capture efficiency of DsRED-MCF-7 cells was increased while the rolling velocity of HL-60 cells was decreased.

## Discussion

This study investigated three phenomena: (i) two proteins with distinct biological functions can be co-immobilized; (ii) rolling and stationary binding of tumor cells can be controlled by immobilized proteins; and (iii) the protein combination enhances the overall capture efficiency of tumor cells.

Tables 1 and 2 demonstrate the co-immobilization of the two proteins. The red fluorescence from APC and the green fluorescence from fluorescein from the surfaces immobilized with either anti-EpCAM or E-selectin have little to no spectral overlap (Supporting Information Figure 1). Furthermore, the even distribution of detected fluorescence (Supporting Information Figure 1) indicates that uniform immobilization of both anti-EpCAM and E-selectin was achieved. The specific correlation between fluorescence and the protein presentation on the slides was confirmed by two experiments. First, the control surfaces treated with BSA exhibited neither red nor green fluorescence, indicating that nonspecific protein adsorption was minimal, which is consistent with a previous report.[33] Second, although E-selectin/APC-anti-EpCAM combinations showed slightly decreased red fluorescence intensities (by ~30%) compared to that for the surfaces functionalized solely with anti-EpCAM at the same concentration, the decrease was marginal. By way of contrast, the green fluorescence intensities from fluorescein-anti-E-selectin substantially increased, in a nonlinear fashion, with an increase in the immobilized amount of E-selectin in the protein mixtures.

Rolling and stationary binding were individually assessed to test the second phenomenon. As shown in Figures 2−4, we have found that the MCF-7 response on different surfaces can be

(33) Brorson, S. H. Bovine serum albumin (BSA) as a reagent against non-specific immunogold labeling on LR-white and epoxy resin. *Micron* **1997**, *28*, 189−195.

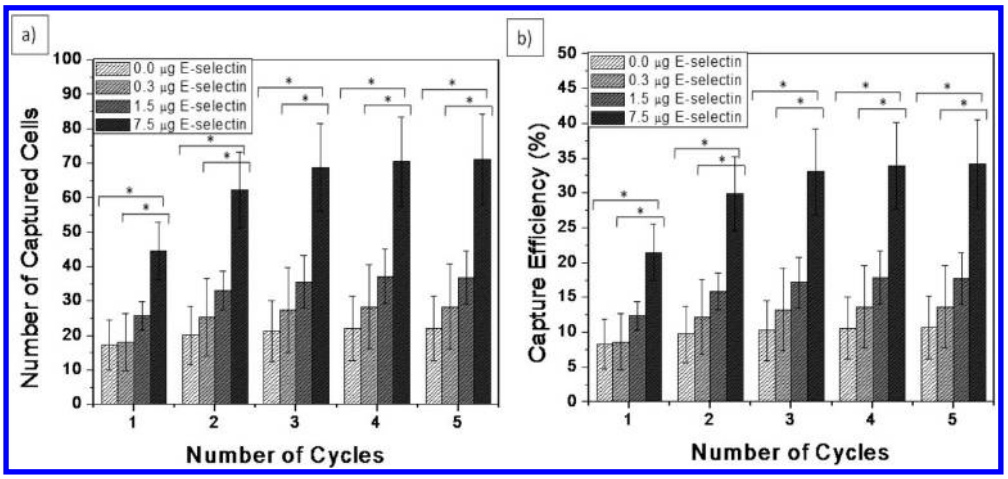


**Figure 6.** (a) Number of captured cells and (b) capture efficiencies of the surfaces immobilized with the mixtures of anti-EpCAM and E-selectin. The number of DsRED-MCF-7 cells on each surface was counted, and the capture efficiency was calculated on the basis of the total number of MCF-7 cells injected into the flow chamber. The flow experiments were performed at a shear stress of 0.16 dyn/cm$^2$. The average capture efficiencies of the surfaces with the mixture of E-selectin and anti-EpCAM were generally higher than those with anti-EpCAM alone. With an increase in E-selectin concentration, the capture efficiency of the surfaces was further enhanced to as high as 3-fold. The measured capture efficiencies were compared by statistical analysis using one-factor ANOVA, followed by Fisher's least significant difference (LSD) tests with 95% simultaneous confidence intervals (SPSS software). Error bars: standard error. *$p < 0.05$.

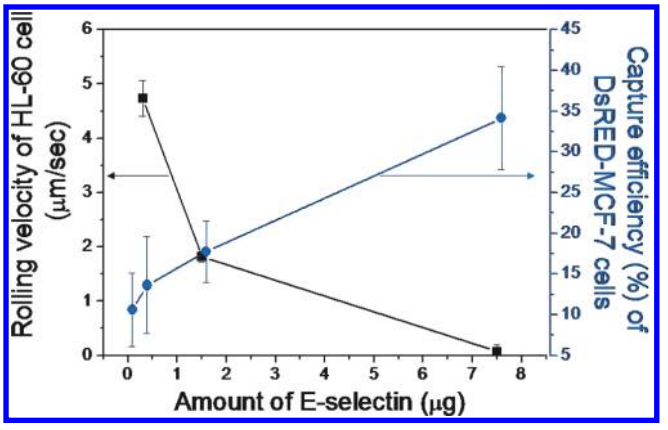


**Figure 7.** Effect of the amount of E-selectin added to an E-selectin /anti-EpCAM mixture on the rolling velocity of HL-60 cells and capture efficiency of DsRED-MCF-7 cells. A mixture of the two cell populations (1:1) was injected onto the surfaces co-immobilized with anti-EpCAM and E-selectin in the presence of anti-IgG at a shear stress of 0.16 dyn/cm$^2$. The amount of immobilized E-selectin was increased from 0, 0.3, and 1.5 to 7.5 $\mu$g, and the amount of immobilized anti-EpCAM was constant at 1.5 $\mu$g. The rolling velocities of HL-60 cells on each slide were 4.74 $\pm$ 0.32 (0.3 $\mu$g), 1.82 $\pm$ 0.10 (1.5 $\mu$g), and 0.07 $\pm$ 0.12 (7.5 $\mu$g of E-selectin) $\mu$m/s. Error bars denote the standard error.

controlled from no interaction (P-selectin) to a rolling response (E-selectin) to stationary binding (anti-EpCAM). The rolling velocities of the HL-60 cells that have a high level of PSGL-1 or sialyl Lewis X (sLe$^x$) expression were less shear-stress-dependent than those of the MCF-7 cells (carcinoma cells).[34] This is most likely caused by the regulation mechanisms by which leukocytic cells such as HL-60 maintain constant rolling velocities under varying flow conditions (Figure 4), whereas carcinoma cells do not.[35,36] Although the transient binding for rolling is a state between firm adhesion and a lack of adhesion (i.e., no interaction), the rolling of leukocytic cells through selectins is very stable because of the high density of selectin ligands present on the leukocytic cells and their resistance against hydrodynamic force applied to the cells.[37] It may be also related to the rigidity of the cells. One can easily imagine that rigid cells are typically more sensitive to shear stress than deformable cells. As a result, leukocytic cells are known to have a nearly constant rolling speed in vivo over a wide range of shear stress.[38] It is also suspected that leukocytic cells maintain a constant rolling speed by shear-dependent compensation mechanisms such as increasing the number of tethers and the number of selectin bonds so that they can be uniformly exposed to activating stimuli.[35] MCF-7 cells (carcinoma cells), however, seem to lack these mechanisms, given that they are more susceptible to changes in shear stress (Figure 4). Moreover, the formation of metastatic cancers often exhibits organ selectivity because of the different interactions between the ligands of cancer cells and the organ-specific selectins of endothelial cells for the extravasation of CTCs, which does not require CTCs to adapt the controlling mechanism of the leukocytic cells.[39]

MCF-7 cells exhibit rolling behavior only on E-selectin, and as reported by Aigner et al.,[34] MCF-7 cells do not interact with P-selectin. Although MCF-7 cells express CD24, a P-selectin ligand, a lack of decoration with sLe$^x$ results in weak interactions that are not strong enough to support stable rolling on P-selectin.[34] E-selectin-mediated rolling of MCF-7 cells under flow was reported by Toezeren et al.[40] In the presence of laminar flow, they reported that the adhesion capacity and rolling

(34) Aigner, S.; Ramos, C. L.; Hafezi-Moghadam, A.; Lawrence, M. B.; Friederichs, J.; Altevogt, P.; Ley, K. CD24 mediates rolling of breast carcinoma cells on P-selectin. *FASEB J.* **1998**, *12*, 1241−1251.

(35) Chen, S.; Springer, T. A. An automatic braking system that stabilizes leukocyte rolling by an increase in selectin bond number with shear. *J. Cell Biol.* **1999**, *144*, 185−200.

(36) Sachs, L. Control of growth and normal differentiation in leukemic cells: regulation of the developmental program and restoration of the normal phenotype in myeloid leukemia. *J. Cell Physiol. Suppl.* **1982**, *1*, 151−164.

(37) Lawrence, M. B.; Springer, T. A. Leukocytes roll on a selectin at physiologic flow rates: distinction from and prerequisite for adhesion through integrins. *Cell* **1991**, *65*, 859−873.

(38) Atherton, A.; Born, G. V. Relationship between the velocity of rolling granulocytes and that of the blood flow in venules. *J. Physiol.* **1973**, *233*, 157−165.

(39) Gout, S.; Tremblay, P. L.; Huot, J. Selectins and selectin ligands in extravasation of cancer cells and organ selectivity of metastasis. *Clin. Exp. Metastasis* **2008**, *25*, 335−344.

(40) Tozeren, A.; Kleinman, H. K.; Grant, D. S.; Morales, D.; Mercurio, A. M.; Byers, S. W. E-selectin-mediated dynamic interactions of breast- and colon-cancer cells with endothelial-cell monolayers. *Int. J. Cancer* **1995**, *60*, 426−431.

behavior of MCF-7 cells on human umbilical endothelial cells (HUVECs) were blocked by treatment with antibodies against E-selectin on the surface of HUVECs, without providing clear evidence. We have shown the clear interaction of MCF-7 cells with immobilized E-selectin in Figure 3, and the behavior of MCF-7 cells was compared with that of HL-60. However, which interaction induces the observed rolling response is still unclear. A ligand of MCF-7 cells against E-selectin needs to be identified because MCF-7 cells lack most of the known ligands against E-selectin such as PSGL-1,[34] CD44,[41] and $sLe^x$.[34] There have been no definitive reports that clearly identify ligands of MCF-7 cells against E-selectin in the literature.

Adherent proteins that are involved in the metastasis process are randomly codistributed on the endothelium.[42] Thus, our hypothesis was that the cooperation of adherent proteins in trapping tumor cells would be more efficient than the activity of one of them alone. The surfaces with the protein mixtures (anti-EpCAM and E-selectin) indeed more efficiently recognize DsRED-MCF-7 cells out of the cell mixture with HL-60 cells than the surfaces functionalized solely with anti-EpCAMs (Figures 5 and 6). The protein combinations used in this study clearly demonstrate great potential for improving the sensitivity and specificity of CTC separation and capture from whole blood. The capture efficiency achieved in this study is as high as approximately 35%. Enhancing the hydrodynamic efficiency of the device will likely further increase the capture efficiency. That is, the introduction of rotation of flow in lieu of the laminar flow that we used in this study will increase the chance for cells to interact with the surface, thereby maximizing the capture efficiency. It was previously reported that microposts in a microfluidic channel[18] or a chaotic mixer[43] substantially increase the interactions between flowing particles (cells) and microfluidic channel surfaces.

One can argue that an increase in E-selectin composition in the protein mixture may lead to the preoccupation of the surface by abundant cells such as leukocytes (HL-60 in this study), resulting in a binding interruption of CTCs (MCF-7 in our study). However, this would not be the case because HL-60 cells exhibit a continuous dynamic rolling response whereas MCF-7 cells remain statically adhered to the surface. That is, a thorough washing step will remove all of the rolling cells, leaving only captured cells behind on the surface. Furthermore, it is shown that the enhanced capture efficiency of MCF-7 cells by the addition of E-selectin to anti-EpCAM is not interrupted by the competitive binding of HL-60 cells. Instead, it is our expectation that E-selectin would be effective in pulling CTCs (MCF-7 cells in this research) along with leukocytes out of the blood, inducing rolling and thereby reducing the velocity of the flowing cells, which would facilitate the stationary binding of CTCs by adjacent anti-EpCAM on the surface. Furthermore, given that cells exhibit significantly different rolling velocities and different levels of interactions with various proteins, the surface responses of different types of cells are expected to be easily controlled by various combinations of proteins. Another potential problem in our CTC detection method as a prognostic tool is that tumor cells are known to alter their adhesiveness and expression of various proteins on their surfaces upon therapeutic intervention.[44] If the surface property alterations result in a substantial decrease in the capture efficiency of our device, then a mix-and-match approach using various ratios between E-selectin and anti-EpCAM would be necessary. That is, a thorough study of the relationship between surface properties of CTCs during treatments and the sensitivity/specificity of various protein combinations should be well understood prior to the implementation of this method in clinics.

Taken together, it is obvious that the addition of E-selectin can induce the rolling of various cell types to be readily accessible by anti-EpCAM, which recognizes/captures tumor cells, resulting in the substantially enhanced capture efficiency of tumor cells by the surface—more than a 3-fold enhancement as compared to that of the surface with anti-EpCAM alone. E-selectin-induced tumor cell rolling most likely maximizes the chance for tumor cells to interact with anti-EpCAM on the surface, resulting in effective stationary binding.

## Conclusions

We have achieved evenly distributed, stable immobilization of proteins (P-selectin, E-selectin, anti-EpCAM, and mixtures of proteins) using epoxy-functionalized glass slides. The immobilized proteins maintained their own biological adhesive functions that induce cell rolling and stationary binding in each specific protein-dependent manner. The patterning and combination of these immobilized proteins as a step toward mimicking physiological complexity can be used to design therapeutic and diagnostic devices for capturing specific cells using their enhanced separation capacity and capture efficiency. We are presently translating these results to a device to capture CTCs from the mixture of other cell lines and whole blood. In addition to the potential use of this device as a metastatic cancer treatment tool by filtering CTCs from the bloodstream, the advantages of this device include the ability to collect CTCs from whole blood under continuous flow without labeling or damaging the CTCs. Therefore, the collected CTCs can be extracted and potentially can be subject to further analysis such as genetic understanding and responses for currently available therapeutic drugs by culture expansion.

**Acknowledgment.** This work was supported by National Science Foundation (NSF) under grant no. CBET-0931472. This investigation was conducted in a facility constructed with support from grant C06RR15482 from the NCRR NIH. We thank Prof. Richard A. Gemeinhart and his group members for optical/fluorescence microscopy measurements and helpful discussion throughout this work.

**Supporting Information Available:** Fluorescence images of functionalized surfaces treated with E-selectin, anti-EpCAM, and E-selectin/anti-EpCAM mixtures in various ratios. This material is available free of charge via the Internet at http://pubs.acs.org.

(41) Zen, K.; Liu, D. Q.; Guo, Y. L.; Wang, C.; Shan, J.; Fang, M.; Zhang, C. Y.; Liu, Y. CD44v4 is a major E-selectin ligand that mediates breast cancer cell transendothelial migration. *PLoS ONE* **2008**, *3*, e1826.

(42) Ley, K.; Laudanna, C.; Cybulsky, M. I.; Nourshargh, S. Getting to the site of inflammation: the leukocyte adhesion cascade updated. *Nat. Rev. Immunol.* **2007**, *7*, 678−689.

(43) Stroock, A. D.; Dertinger, S. K.; Ajdari, A.; Mezic, I.; Stone, H. A.; Whitesides, G. M. Chaotic mixer for microchannels. *Science* **2002**, *295*, 647−651.

(44) Kiani, M. F.; Fenton, B. M.; Sporn, L. A.; Siemann, D. W. Effects of ionizing radiation on the adhesive interaction of human tumor and endothelial cells in vitro. *Clin. Exp. Metastasis* **1997**, *15*, 12−18.